Surface lattice solitons

Konstantinos G. Makris, Jared Hudock, Demetrios N. Christodoulides, and George I. Stegeman

College of Optics/CREOL, University of Central Florida, Orlando, Florida 32816

Ofer Manela and Mordechai Segev

Department of Physics, Technion-Israel Institute of Technology, Haifa 32000, Israel

Received February 27, 2006; revised April 7, 2006; accepted June 2, 2006;
posted July 10, 2006 (Doc. ID 68529); published August 25, 2006

We study theoretically nonlinear surface waves in optical lattices and show that solitons can exist at the heterointerface between two different semi-infinite 1D waveguide arrays, as well as at the boundaries of a 2D nonlinear lattice. The existence and properties of these surface soliton solutions are investigated in detail. © 2006 Optical Society of America

OCIS codes: 190.4350, 190.4390.

Surface waves are, by their very nature, guided waves propagating along the interface of two different media.[1] In the linear optical domain, such surface waves can exist between a metal and a dielectric (plasmon waves) and at the boundary of two semi-infinite periodic dielectric media,[2] as well as at the interfaces of anisotropic materials. In addition to these families of linear waves, optical surface waves can also arise from nonlinearity, e.g., at the interface between a linear medium and a nonlinear material.[3–5] Yet, as of today, only diffusion-induced nonlinear surface waves have been reported,[6] primarily because of fabrication and experimental difficulties (surface roughness etc.). However, many of these practical problems can be overcome by using nonlinear waveguide arrays instead.[7] These periodic topologies are known to exhibit novel properties in both the linear and the nonlinear optical regimes and have been extensively studied during the past few years.[8] More specifically, modulation instability[9] and discrete or lattice solitons in cubic,[10–13] photorefractive,[14,15] and quadratic waveguide arrays[16] have been examined theoretically and observed experimentally. Very recently, surface wave lattice solitons occurring at the boundaries of optical lattices were predicted[17] and experimentally observed[18] as a new class of self-trapped surface states.

In this Letter we study nonlinear surface waves in 1D and 2D optical lattices and predict surface lattice solitons propagating along the heterointerface of two different semi-infinite waveguide arrays. A unique characteristic of this new family of solitons is that two different semi-infinite field profiles can form a composite entity, namely a *hybrid* surface soliton. We investigate several generic examples of hybrid surface solitons residing in different bandgaps of the composite heterostructure and study their stability. Finally, we predict surface lattice solitons occurring at the boundaries of a 2D lattice (at a corner or at an edge) when their power level is above a critical threshold.

Let us consider a lattice consisting of two different semi-infinite waveguide arrays, as shown in Fig. 1. Every waveguide is designed to be single mode, and the assumed nonlinearity is of the self-focusing or defocusing Kerr type. Since the difference in the refractive indices (with respect to the cladding) is small, a scalar approach is applicable for the particular problem. In this case, the system is governed by a paraxial scalar nonlinear Schrödinger equation capable of describing higher-order band dynamics. In normalized units this equation is written as

$$i\frac{\partial u}{\partial z}+\frac{\partial^2 u}{\partial x^2}+V(x)u+\sigma|u|^2u=0, \tag{1}$$

where $u(x,z)$ is the slowly varying envelope of the optical field, $V(x)$ is the index potential that describes the composite structure of the two semi-infinite waveguide arrays, and the coefficient σ is $\sigma=+1$ (-1) for self-focusing (defocusing) nonlinearities. For demonstration purposes, let both regions in Fig. 1 have a linear refractive index difference of 2.8×10^{-3}, with equally spaced sites (10 μm center to center). Note that the difference between the width of the channels leads to an effective mismatch in the propagation constant in the two regions. As a result, the bands of the right and left arrays are relatively shifted, as can be seen in Fig. 2. If this shift is large enough, solitons whose propagation eigenvalues reside inside a forbidden gap are possible. It can be formally shown that the band structure of the entire heterointerface involves the individual band structures of each of the two semi-infinite optical lattices, which in turn are related to the band diagrams of the corresponding infinite arrays. Figure 2 also demonstrates that for the specific design parameters used here, there is a band overlap between the second and the third band of the two different semi-infinite arrays. Therefore soliton solutions can be obtained only in the resulting three complete bandgaps. More spe-

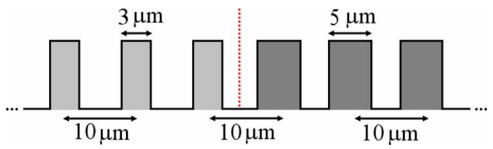

Fig. 1. Two semi-infinite waveguide arrays joined together.

0146-9592/06/182774-3/$15.00

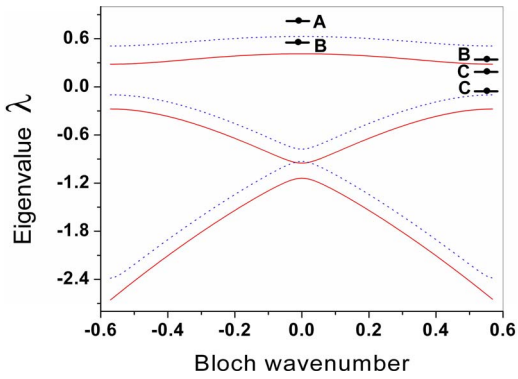

Fig. 2. Band structure of the two coupled semi-infinite waveguide arrays. The dotted curves correspond to the band structure of the right-hand array, while the solid curves correspond to that of the left-hand array. Points A, B, and C represent the propagation eigenvalues of the allowed surface solitons.

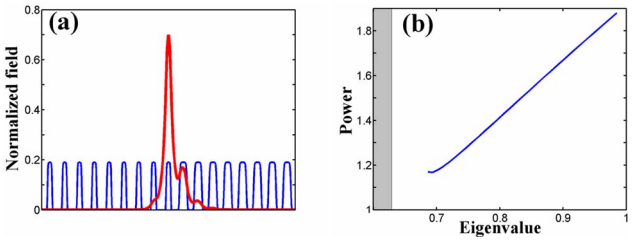

Fig. 3. (a) Field profile of a hybrid in-phase–in-phase soliton and (b) the corresponding power–eigenvalue diagram. The gray areas represent the bands of the structure.

cifically, one can identify surface solitons with propagation constants in the semi-infinite gap, in the first gap between the two first bands and in the second gap between the first band of the left-hand array and the second band of the right-hand array (points A, B, and C, respectively, in Fig. 2). It is important to note that the hybrid solitons are a direct outcome of the nonlinearity, since the heterostructure does not support linear defect modes and does not lead to pinned states owing to inhomogeneities. In all cases the lattice surface solitons are numerically found by using numerical relaxation schemes based on the self-consistent method.[11] This is done by assuming stationary solutions of the form $u(x,z)=\phi(x)\exp(i\lambda z)$, where $\phi(x)$ is the field profile and λ is the nonlinear correction to the propagation constant or the soliton eigenvalue.

Figure 3(a) depicts the field profile of a surface soliton existing at the nonlinear heterointerface of Fig. 1. This soliton state corresponds to the eigenvalue A of Fig. 2, which is located in the semi-infinite bandgap of both lattices. As a result, the two components comprising this soliton are in phase. The power-eigenvalue stability diagram ($P-\lambda$ curve) associated with this solution is shown in Fig. 3(b). This curve terminates close to $\lambda \approx 0.69$, which is close to the top edge of the first band of the right array. In this region the solutions start to become unstable, as one may also anticipate from the Vakhitov–Kolokolov criterion. For higher eigenvalues these solutions are stable.

Another interesting case arises when the soliton eigenvalue is located at point B of Fig. 2. This implies that B is at the top of the first band (in the semi-infinite bandgap) of the left-hand array and at the bottom of the first band (first bandgap) of the right-hand lattice. Therefore one part of the surface soliton field in the left-hand array will be in phase, whereas the other part on the right-hand array will be staggered (the field lobes are π out of phase). As a result, the two components can propagate locked together as a composite self-trapped state, thus forming a hybrid surface soliton. A typical field profile of this type of hybrid soliton is shown in Fig. 4(a). The power of these hybrid solutions with respect to the corresponding soliton eigenvalue λ is plotted in Fig. 4(c). As the eigenvalue λ approaches the edge of the first band (of the right array) the staggered component of the solution becomes wider while the in-phase component is getting more localized. The converse occurs when the eigenvalue λ is close to the edge of the second band. The stability of this solution was investigated by using beam propagation methods. Another solution can be found in the third complete gap (eigenvalue C in Fig. 2) when the nonlinearity is of the defocusing type ($\sigma=-1$). The field profile of this surface soliton as well as the associated $P-\lambda$ are shown in Figs. 4(b) and 4(d), respectively. In this latter case, both components at the interface are of the staggered type.

Surface solitons can also exist at the boundaries of 2D lattices. More specifically, we have examined a nonlinear Kerr semi-infinite square lattice of waveguides. The linear refractive index between the core and the cladding is taken here to be 4×10^{-3}, and the distance between the single-mode waveguides is 6 μm in both orthogonal directions. The wave propagation in this 2D self-focusing optical lattice is described by the normalized nonlinear Schrödinger equation

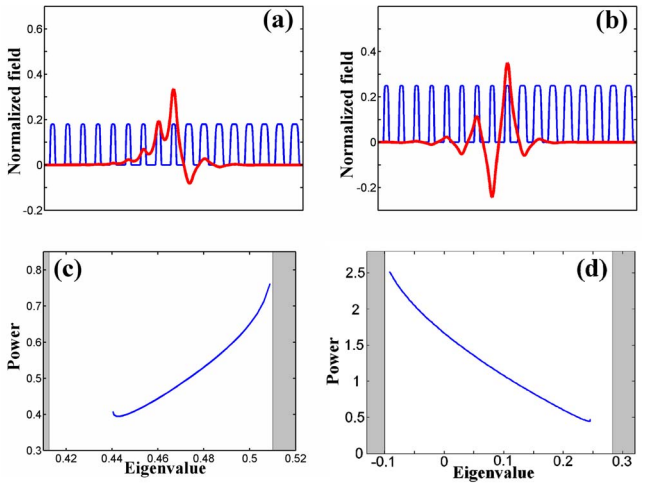

Fig. 4. Field profile of a hybrid (a) in-phase–staggered soliton, and (b) staggered–staggered soliton. The powers–eigenvalue diagrams for these solutions are depicted in (c) and (d), respectively. The gray areas represent the bands of the structure.

$$i\frac{\partial u}{\partial z} + \frac{\partial^2 u}{\partial x^2} + \frac{\partial^2 u}{\partial y^2} + V(x,y)u + |u|^2 u = 0, \qquad (2)$$

where $V(x,y)$ is the semi-infinite index potential. Our analysis leads to new soliton solutions existing at the corner [see Fig. 5(a)] and at the edge [see Fig. 5(b)] of the 2D lattice. The power associated with these surface solitons is plotted in Fig. 5(c) as a function of the corresponding eigenvalue λ. Our analysis shows that both these soliton solutions are possible only when their power exceeds a critical threshold. The threshold of the edge surface state is slightly higher than that of the corner soliton, which is physically anticipated, since the latter self-trapped state is confined in fewer sites. In both cases, the propagation constants of these surface solitons are located at the semi-infinite bandgap of the lattice. Before closing, we would like to mention that other surface soliton configurations may also be possible, such as, for example, gap surface solitons in both 1D and 2D arrangements.[19]

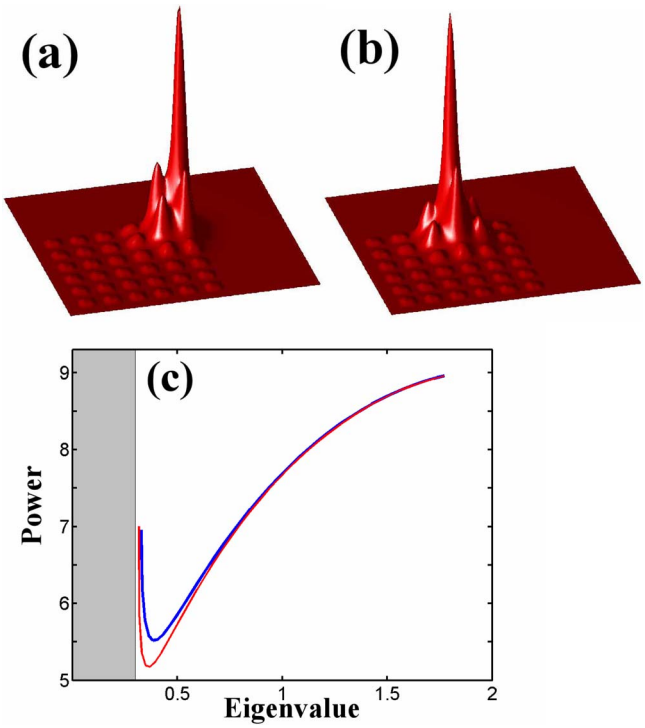

Fig. 5. Intensities of surface solitons in a semi-infinite square lattice located at (a) the corner, and (b) at the edge of the 90° angular sector lattice. The corresponding power–eigenvalues diagrams are shown in (c) for the corner (thin curve) and edge (thick curve) surface lattice solitons. The gray area represents the first band of the 2D array.

In conclusion we have theoretically demonstrated the existence of surface spatial solitons in nonlinear optical lattices. Such surface self-trapped waves can exist at the interface between two different semi-infinite 1D waveguide arrays as well as at the boundaries of 2D optical lattices. The stability of these states was also investigated.

References

1. S. G. Davison and M. Steslicka, *Basic Theory of Surface States* (Oxford U. Press, 1992).
2. P. Yeh, A. Yariv, and A. Y. Cho, Appl. Phys. Lett. **32**, 104 (1978).
3. N. N. Akhmediev, V. I. Korneev, and Y. V. Kuz'menko, Sov. Phys. JETP **61**, 62 (1985).
4. U. Langbein, F. Lederer, and H. E. Ponath, Opt. Commun. **46**, 167 (1983).
5. C. T. Seaton, J. D. Valera, R. L. Shoemaker, G. I. Stegeman, J. T. Chilwell, and S. D. Smith, IEEE J. Quantum Electron. **21**, 782 (1985).
6. M. Cronin-Golomb, Opt. Lett. **20**, 2075 (1995).
7. D. N. Christodoulides and R. I. Joseph, Opt. Lett. **13**, 794 (1988).
8. D. N. Christodoulides, F. Lederer, and Y. Silberberg, Nature **424**, 817 (2003).
9. J. Meier, G. I. Stegeman, D. N. Christodoulides, Y. Silberberg, R. Morandotti, H. Yang, G. Salamo, M. Sorel, and J. S. Aitchison, Phys. Rev. Lett. **92**, 163902 (2004).
10. H. S. Eisenberg, Y. Silberberg, R. Morandotti, and J. S. Aitchison, Phys. Rev. Lett. **81**, 3383 (1998).
11. O. Cohen, T. Schwartz, J. W. Fleischer, M. Segev, and D. N. Christodoulides, Phys. Rev. Lett. **91**, 113901 (2003).
12. Z. Musslimani and J. Yang, J. Opt. Soc. Am. B **21**, 973 (2004).
13. O. Cohen, G. Bartal, H. Buljan, T. Carmon, J. W. Fleischer, M. Segev, and D. N. Christodoulides, Nature **433**, 500 (2005).
14. J. W. Fleischer, M. Segev, N. K. Efremidis, and D. N. Christodoulides, Nature **422**, 147 (2003).
15. N. K. Efremidis, J. Hudock, D. N. Christodoulides, J. W. Fleischer, O. Cohen, and M. Segev, Phys. Rev. Lett. **91**, 213906 (2003).
16. R. Iwanow, R. Schiek, G. I. Stegeman, T. Pertsch, F. Lederer, Y. Min, and W. Sohler, Phys. Rev. Lett. **93**, 113902 (2004).
17. K. G. Makris, S. Suntsov, D. N. Christodoulides, G. I. Stegeman, and A. Hache, Opt. Lett. **30**, 2466 (2005).
18. S. Suntsov, K. G. Makris, D. N. Christodoulides, G. I. Stegeman, A. Haché, R. Morandotti, H. Yang, G. Salamo, and M. Sorel, Phys. Rev. Lett. **96**, 063901 (2006).
19. Y. Kartashov, L. Torner, and V. A. Vysloukh, Phys. Rev. Lett. **96**, 073901 (2006).